



A comparative study of dark matter flow & hydrodynamic turbulence and its applications

May 2022

Zhijie (Jay) Xu

Multiscale Modeling Team
Computational Mathematics Group
Physical & Computational Science Directorate
Zhijie.xu@pnnl.gov; zhijiexu@hotmail.com



PNNL is operated by Battelle for the U.S. Department of Energy



Pacific
Northwest
NATIONAL LABORATORY

Preface

Dark matter, if exists, accounts for five times as much as ordinary baryonic matter. Therefore, dark matter flow might possess the widest presence in our universe. The other form of flow, hydrodynamic turbulence in air and water, is without doubt the most familiar flow in our daily life. During the pandemic, we have found time to think about and put together a systematic comparison for the connections and differences between two types of flow, both of which are typical non-equilibrium systems.

The goal of this presentation is to leverage this comparison for a better understanding of the nature of dark matter and its flow behavior on all scales. Science should be open. All comments are welcome.

Thank you!

Data repository and relevant publications

Structural (halo-based) approach:

0.	Data https://dx.doi.org/10.5281/zenodo.6541230
1.	Inverse mass cascade in dark matter flow and effects on halo mass functions https://doi.org/10.48550/arXiv.2109.09985
2.	Inverse mass cascade in dark matter flow and effects on halo deformation, energy, size, and density profiles https://doi.org/10.48550/arXiv.2109.12244
3.	Inverse energy cascade in self-gravitating collisionless dark matter flow and effects of halo shape https://doi.org/10.48550/arXiv.2110.13885
4.	The mean flow, velocity dispersion, energy transfer and evolution of rotating and growing dark matter halos https://doi.org/10.48550/arXiv.2201.12665
5.	Two-body collapse model for gravitational collapse of dark matter and generalized stable clustering hypothesis for pairwise velocity https://doi.org/10.48550/arXiv.2110.05784
6.	Evolution of energy, momentum, and spin parameter in dark matter flow and integral constants of motion https://doi.org/10.48550/arXiv.2202.04054
7.	The maximum entropy distributions of velocity, speed, and energy from statistical mechanics of dark matter flow https://doi.org/10.48550/arXiv.2110.03126
8.	Halo mass functions from maximum entropy distributions in collisionless dark matter flow https://doi.org/10.48550/arXiv.2110.09676

Statistics (correlation-based) approach:

0.	Data https://dx.doi.org/10.5281/zenodo.6569898
1.	The statistical theory of dark matter flow for velocity, density, and potential fields https://doi.org/10.48550/arXiv.2202.00910
2.	The statistical theory of dark matter flow and high order kinematic and dynamic relations for velocity and density correlations https://doi.org/10.48550/arXiv.2202.02991
3.	The scale and redshift variation of density and velocity distributions in dark matter flow and two-thirds law for pairwise velocity https://doi.org/10.48550/arXiv.2202.06515
4.	Dark matter particle mass and properties from two-thirds law and energy cascade in dark matter flow https://doi.org/10.48550/arXiv.2202.07240
5.	The origin of MOND acceleration and deep-MOND from acceleration fluctuation and energy cascade in dark matter flow https://doi.org/10.48550/arXiv.2203.05606
6.	The baryonic-to-halo mass relation from mass and energy cascade in dark matter flow https://doi.org/10.48550/arXiv.2203.06899

Structural (halo-based) approach for dark matter flow

The mean flow, velocity dispersion, energy transfer and evolution of rotating & growing dark matter halos

Xu Z., 2022, arXiv:2201.12665 [astro-ph.GA]
<https://doi.org/10.48550/arXiv.2201.12665>

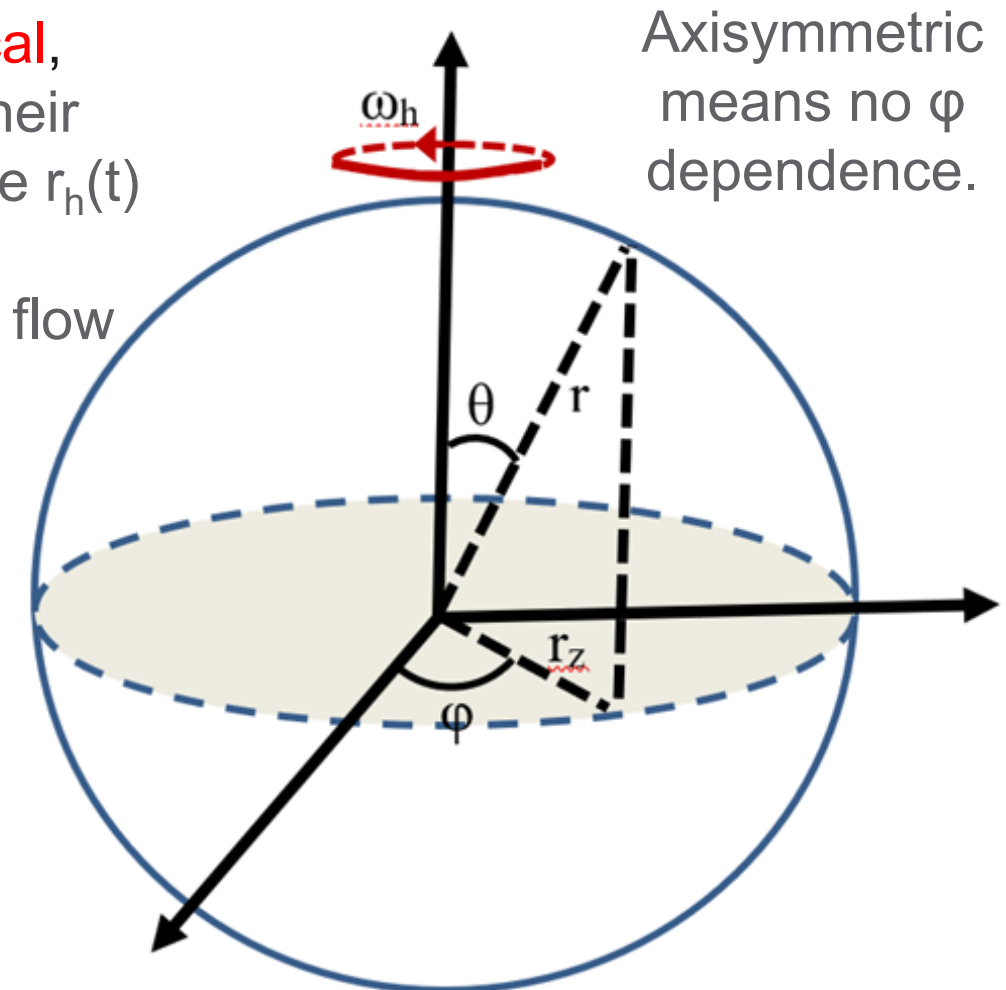
Introduction

Review: In hydrodynamic turbulence, “Reynolds stress” facilitates the **one-way** energy exchange from coherent (mean) flow to random fluctuation (turbulence) and enhances system entropy.

Existing study of halos mostly focus on the **spherical non-rotating non-growing** halos with a vanishing radial flow (fully virialized halos with slow mass accretion in their late stage).

- Goal 1: Explore solutions of mean flow and dispersions for **spherical**, **axisymmetric**, **growing** and **rotating** halos (fast mass accretion in their early stage) with an effective angular velocity $\omega_h(t)$ and varying size $r_h(t)$
- Goal 2: Explore the transition of halos from early to late stage
- Goal 3: Explore the role of halos in energy transfer between mean flow and random fluctuation.

Density:	$\rho_h = \rho_h(r, t)$	Potential:	$\phi_r = \phi_r(r, t)$
Radial flow:	$u_r = u_r(r, t)$		$\sigma_{rr}^2 = \sigma_{rr}^2(r, \theta, t)$
The polar flow (meridional flow):	$u_\theta = u_\theta(r, \theta, t)$		$\sigma_{\theta\theta}^2 = \sigma_{\theta\theta}^2(r, \theta, t)$
azimuthal flow (zonal flow):	$u_\phi = u_\phi(r, \theta, t)$		$\sigma_{\phi\phi}^2 = \sigma_{\phi\phi}^2(r, \theta, t)$



Reduced equations and anisotropic parameter

The continuity equation reduces to:

$$\frac{\partial \rho_h}{\partial t} + \frac{1}{r^2} \frac{\partial (r^2 \rho_h u_r)}{\partial r} = 0$$

Six equations and 8 Variables; need extra closures to solve;

Observations of flow on rotating sphere strongly suggest that as the rotation rate increases, the azimuthal flow becomes dominant and the **polar flow may be neglected**.

With $u_\theta \approx 0$ and $\sigma_{r\theta}^2 = \sigma_{r\phi}^2 = \sigma_{\phi\theta}^2 = 0$

The full momentum equations (Jeans' equation) reduces to

$$\frac{\partial u_r}{\partial t} + u_r \frac{\partial u_r}{\partial r} + \frac{1}{\rho_h} \frac{\partial (\rho_h \sigma_{rr}^2)}{\partial r} + \frac{2}{r} \sigma_{rr}^2 \left(1 - \frac{\sigma_{\theta\theta}^2 + \sigma_{\phi\phi}^2 + u_\phi^2}{2\sigma_{rr}^2} \right) + \frac{\partial \phi_r}{\partial r} = 0$$

For θ : $u_\phi^2 = \sigma_{\theta\theta}^2 - \sigma_{\phi\phi}^2 + \frac{\sin \theta}{\cos \theta} \frac{\partial \sigma_{\theta\theta}^2}{\partial \theta}$

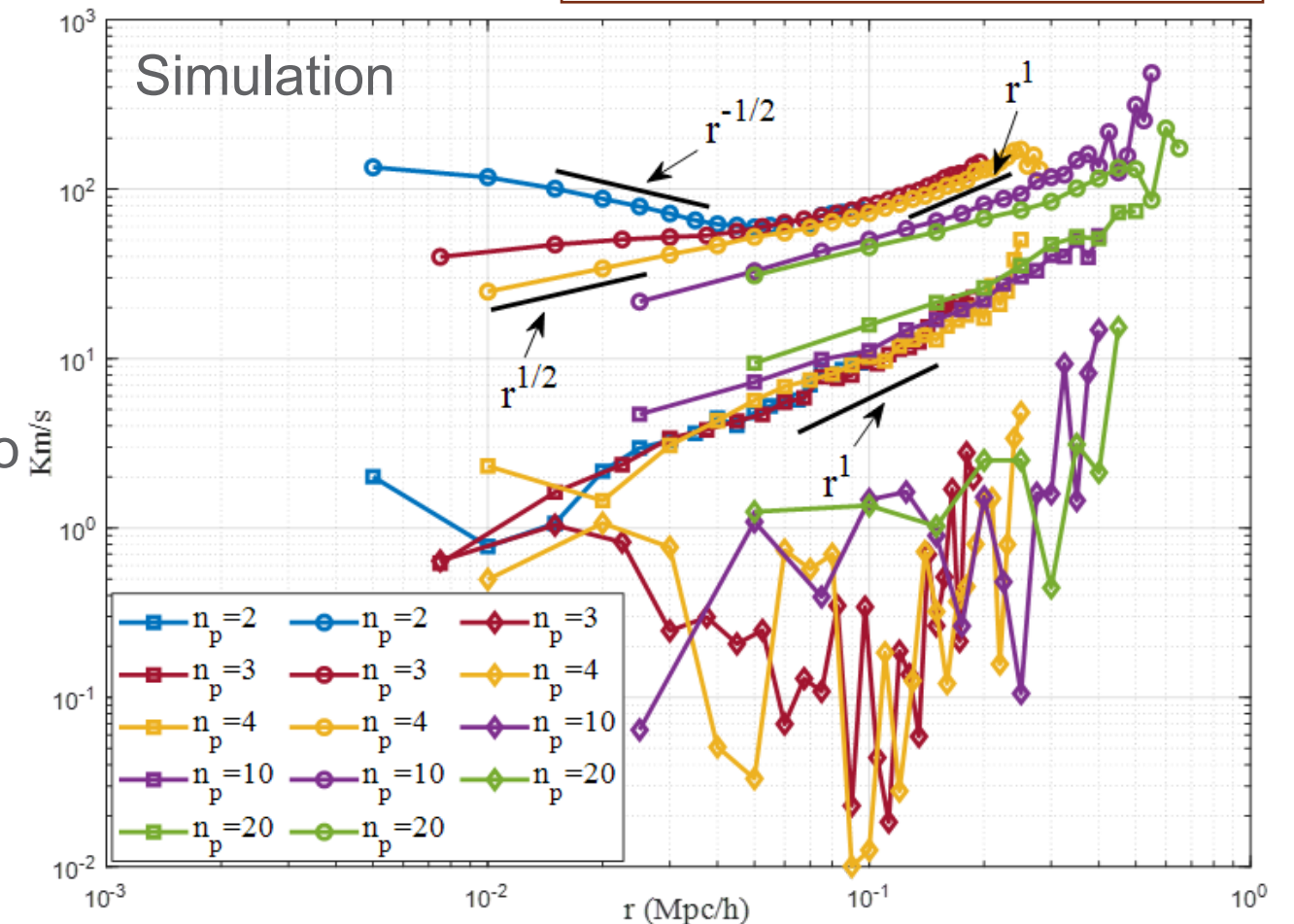
For ϕ : $\frac{\partial u_\phi}{\partial t} + u_r \frac{\partial u_\phi}{\partial r} + \frac{u_r u_\phi}{r} = 0$

$$\frac{\partial \phi_r}{\partial r} = \frac{Gm_r(r,t)}{r^2}$$

$$\rho_h = \frac{1}{4\pi r^2} \frac{\partial m_r(r,t)}{\partial r}$$

Anisotropic parameter should include effect of u_ϕ or centripetal force:

$$\beta_h = 1 - \frac{\sigma_{\theta\theta}^2 + \sigma_{\phi\phi}^2}{2\sigma_{rr}^2} \text{ Old} \quad \beta_{h1} = 1 - \frac{\sigma_{\theta\theta}^2 + \sigma_{\phi\phi}^2 + u_\phi^2}{2\sigma_{rr}^2} \text{ New}$$



Circle: u_ϕ ; Square: radial flow u_{rp} ; Diamond: u_θ

Polar flow can be neglected

Evolution of halo angular momentum

From continuity and momentum equations:

$$\frac{\partial(\rho_h u_\phi)}{\partial t} + \frac{1}{r^2} \frac{\partial[(\rho_h u_\phi) u_r r^2]}{\partial r} + \frac{u_r}{r} (\rho_h u_\phi) = 0$$

The halo angular momentum is:

$$\bar{H}_h = \int_0^{r_h} 2\pi r^3 \rho_h(r) \left(\int_0^\pi u_\phi \sin^2 \theta d\theta \right) dr$$

Time evolution of angular momentum:

$$\frac{\partial \bar{H}_h}{\partial t} = 2\pi r_h^3 \rho_h(r_h) \int_0^\pi u_\phi(r_h, \theta) \sin^2 \theta d\theta \left(\frac{\partial r_h}{\partial t} - u_r(r_h) \right)$$

The halo angular momentum is conserved only if

$$\frac{\partial r_h}{\partial t} = u_r(r_h)$$

However, for growing halos

$$\begin{matrix} \frac{\partial r_h}{\partial t} > 0 \\ u_r(r_h) \leq 0 \end{matrix} \Rightarrow \frac{\partial \bar{H}_h}{\partial t} > 0$$

- In hydrodynamic turbulence, angular momentum is conserved during vortex stretching.
- In dark matter flow, halo angular momentum is not conserved and always increasing with time.
- The Tidal Torque Theory (TTT) relates the angular momentum to the misalignment between the tidal shear field and halo shape.
- TTT predicts a linear increase with time t for halo with a fixed given mass $\bar{H}_h \sim t$
- A growing halo may obtain its momentum through continuous mass acquisition and $\bar{H}_h \sim t^2$

Evolution of halo rotational kinetic energy

From continuity and momentum equations:

$$\underbrace{\frac{\partial(\rho_h u_\varphi^2)}{\partial t}}_{\text{derivative}} + \underbrace{\frac{1}{r^2} \frac{\partial[(\rho_h u_\varphi^2) u_r r^2]}{\partial r}}_{\text{advection}} + \underbrace{2 \rho_h u_\varphi^2 \frac{u_r}{r}}_{\text{production}} = 0$$



The halo rotational kinetic energy is obtained by integration:

$$\bar{K}_a = \frac{1}{2} \int_0^{r_h} 2\pi r^2 \int_0^\pi (\rho_h u_\varphi^2) \sin \theta d\theta dr$$



Time evolution of rotational kinetic energy:

$$\frac{\partial \bar{K}_a}{\partial t} = \underbrace{\pi r_h^2 \rho_h(r_h) \int_0^\pi u_\varphi^2(r_h, \theta) \sin \theta d\theta \left(\frac{\partial r_h}{\partial t} - u_r(r_h) \right)}_1 - \underbrace{\int_0^{r_h} 2\pi r^2 \frac{u_r}{r} \rho_h \left(\int_0^\pi u_\varphi^2 \sin \theta d\theta \right) dr}_2$$

1: surface contribution from mass cascade

2: bulk cont. from energy transfer

- In hydrodynamic turbulence, the “Reynolds” stress facilitates the **one-way** energy exchange from coherent (mean) flow to random fluctuation and enhances entropy.
- In dark matter flow, the production term describes the fictitious stress acting on the gradient of mean radial flow to facilitate the energy transfer between mean azimuthal flow and random fluctuation.
- Since u_r is positive in core region and negative in outer region, the energy transfer is **two-way**, i.e. energy is drawn from random motion to mean flow in outer region and from mean flow to random motion in core region.
- However, for entire halo, there is a net transfer from mean flow to random flow to enhance the halo entropy.

General solutions for rotating, and growing halos

Key: decomposition of velocity dispersion:

Introduce reduced spatial/temporal coordinate: $x(r, t) = \frac{r}{r_s(t)} = \frac{cr}{r_h(t)}$

$$\sigma_{\theta\theta}^2(r, \theta, t) = \underbrace{\sigma_{r0}^2(r, t)}_1 + \underbrace{\alpha_\phi(r, t) u_\phi^2(r, \theta, t)}_2$$

1: Axial-dispersion 2: Spin-dispersion

$$\sigma_{\phi\phi}^2(r, \theta, t) = \sigma_{r0}^2(r, t) + \beta_\phi(r, t) u_\phi^2(r, \theta, t)$$

$$\sigma_{rr}^2(r, \theta, t) = \sigma_{r0}^2(r, t) + \gamma_\phi(r, t) u_\phi^2(r, \theta, t)$$

Momentum equation for θ :

$$\frac{\partial u_\phi}{\partial t} + u_r \frac{\partial u_\phi}{\partial r} + \frac{u_r u_\phi}{r} = 0$$

Momentum equation for ϕ :

$$u_\phi^2 = \sigma_{\theta\theta}^2 - \sigma_{\phi\phi}^2 + \frac{\sin \theta}{\cos \theta} \frac{\partial \sigma_{\theta\theta}^2}{\partial \theta}$$

Separation of variables:

$$u_\phi(r, \theta, t) = \omega_h(t) r_s(t) F_\phi(x) K_\phi(\theta)$$

$$\sigma_{rr}^2(r, \theta = 0, t) = \sigma_{\theta\theta}^2(r, \theta = 0, t) = \sigma_{\phi\phi}^2(r, \theta = 0, t) = \sigma_{r0}^2(r, t)$$

- Spin causes velocity anisotropy; Velocity dispersions can be expressed as a function of azimuthal flow u_ϕ .
- Velocity dispersion is expected to be isotropic for non-rotating halos with a spherical symmetry.
- For spherical halos with a finite spin, velocity dispersions are only isotropic along the axis of rotation ($\theta=0$)

Halo spin

$$\frac{\partial \ln F_\phi}{\partial \ln x} = \frac{u_h(x) + x \left(\frac{\partial \ln \omega_h}{\partial \ln t} + \frac{\partial \ln r_s}{\partial \ln t} \right)}{x \frac{\partial \ln r_s}{\partial \ln t} - u_h(x)}$$

Mass cascade

Radial flow

$$K_\phi(\theta) = (\sin \theta)^{\alpha_\theta} \quad \text{with an angular exponent}$$

$$\alpha_\theta = \frac{1 + \beta_\phi - \alpha_\phi}{2\alpha_\phi}$$

General solutions for rotating, and growing halos

Momentum equation for r:
$$\frac{\partial u_r}{\partial t} + u_r \frac{\partial u_r}{\partial r} + \frac{1}{\rho_h} \frac{\partial (\rho_h \sigma_{rr}^2)}{\partial r} + \frac{2}{r} \sigma_{rr}^2 \left(1 - \frac{\sigma_{\theta\theta}^2 + \sigma_{\phi\phi}^2 + u_\phi^2}{2\sigma_{rr}^2} \right) + \frac{\partial \phi_r}{\partial r} = 0$$

Equation for axial-dispersion:

$$\frac{\partial u_r}{\partial t} + u_r \frac{\partial u_r}{\partial r} + \frac{1}{\rho_h} \frac{\partial (\rho_h \sigma_{r0}^2)}{\partial r} + \frac{\partial \phi_r}{\partial r} + F_a(r, t) = 0$$

Equation for spin-dispersion:

$$\frac{\partial \ln(\gamma_\phi u_\phi^2)}{\partial \ln x} + \frac{\partial \ln \rho_h}{\partial \ln x} + 2 - 2\alpha_a = \frac{rF_a(r, t)}{\gamma_\phi u_\phi^2}$$

The coupling function reflects the coupling between **axial-dispersion** and **spin-dispersion**

Two anisotropy parameters are related:

$$\beta_{h1} = \frac{1 - \alpha_a}{1 + \sigma_{r0}^2 / (\gamma_\phi u_\phi^2)}$$

$$\alpha_a = \frac{(\alpha_\phi + \beta_\phi + 1)}{2\gamma_\phi}$$

For virialized “small” halos with slow mass accretion (late stage), the axial- and spin-dispersions are decoupled.

Axial-dispersion is dominant to balance gravity.

$$F_a(r, t) = 0 \quad \text{and} \quad \sigma_{r0}^2 \gg \gamma_\phi u_\phi^2 \rightarrow \beta_{h1} \approx 0$$

For “large” halos with fast mass accretion (early stage), the axial- and spin-dispersions are decoupled.

Spin-dispersion is dominant to balance gravity.

$$F_a(r, t) \approx -\frac{\partial \phi_r}{\partial r} \quad \text{and} \quad \sigma_{r0}^2 \ll \gamma_\phi u_\phi^2 \rightarrow \beta_{h1} \approx 1 - \alpha_a$$

Two limiting situations: “small” and “large” halos

We still require a clear definition of “small” and “large” halos.

Enclose mass within radius r

$$m_r(r, t) = m_h(t) \frac{F(x)}{F(c)}$$

Halo density

$$\rho_h(r, t) = \frac{m_h(t)}{4\pi r_s^3} \frac{F'(x)}{x^2 F(c)}$$

The ratio of core mass to halo mass:

$$C_F = \frac{F(1)}{F(c)} = \frac{m_r(r_s, t)}{m_h(t)}$$

Peak height:

$$v = \delta_{cr} / \sigma(m_h, z)$$

From spherical collapse model

$$\delta_{cr} \approx 1.68$$

σ is (root mean square) fluctuation of the smoothed density

At same redshift z , large halos has higher v

Properties of “large” halos:

- Early stage of halo life with high peak height v
- Extremely fast mass accretion
- A growing core with scale radius $r_s \sim t$
- Growing halo size $r_h \sim t$ and halo mass $m_h \sim t$
- Constant halo concentration $c \approx 3.5$ (limiting c)

Properties of “small” halos:

- Late stage of halo life with low peak height v
- Extremely slow mass accretion
- A stable core, constant scale radius r_s , and constant core-to-halo mass ratio C_F
- Increasing concentration $c \sim t^{2/3} \sim a$ and $m_h \sim F(c)$

Solutions for “small” halos at late stage

Coupling function:

$$F_a(r, t) = 0$$

Mean flow:

$$u_r = u_\theta = 0$$

Velocity dispersions:

$$\sigma_{rr}^2 = \sigma_{\phi\phi}^2 = \sigma_{\theta\theta}^2 + u_\phi^2$$

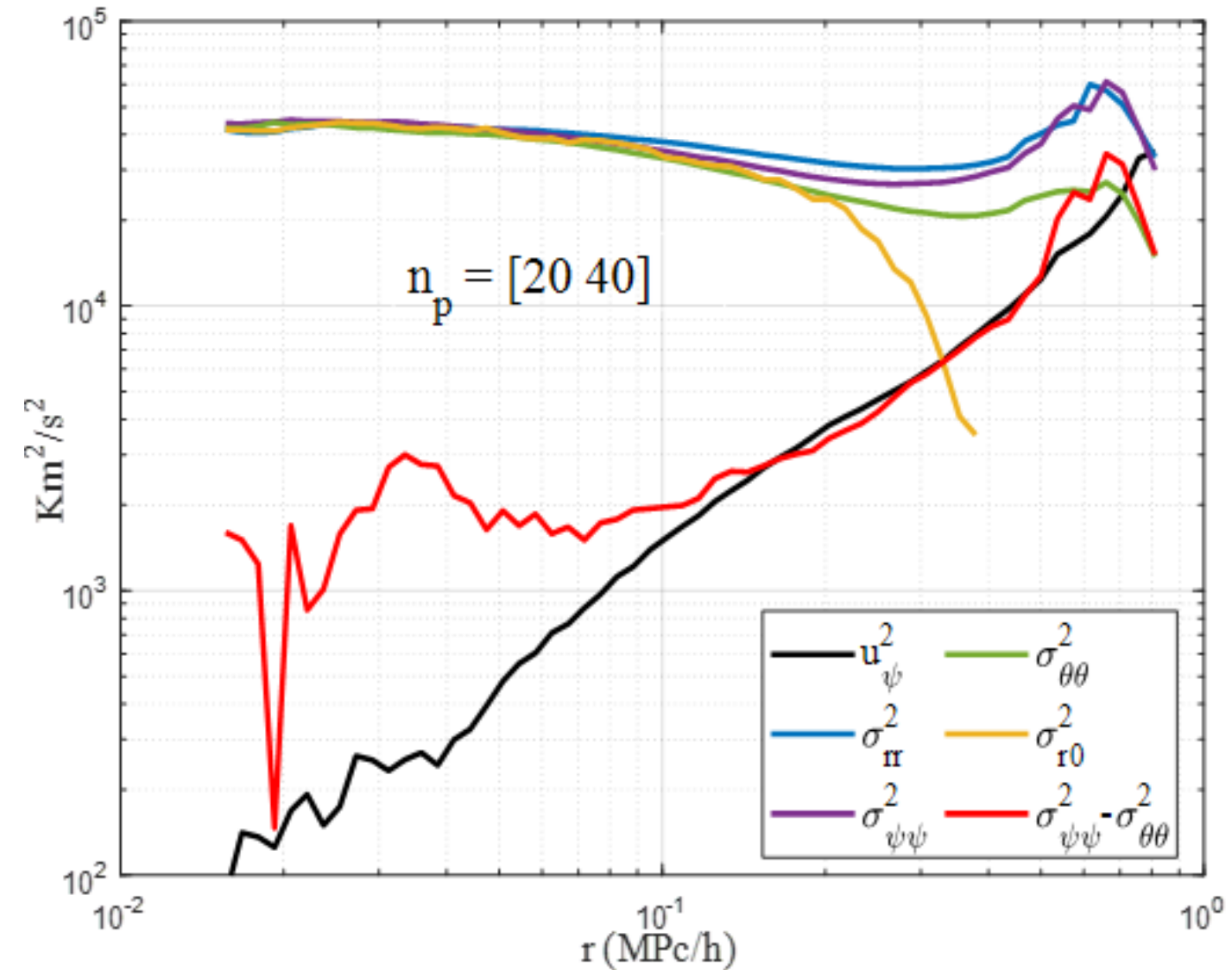
Anisotropy parameters : $\alpha_a = 1$ $\beta_{h1} = 0$

Angular exponent : $\alpha_\theta = 1$

$$1 + \alpha_\phi = \beta_\phi = \gamma_\phi \quad \alpha_\phi = 1 \quad \beta_\phi = \gamma_\phi = 2$$

Properties of “small” halos (continued):

- Virialized and bound with vanishing radial flow
- Incompressible (proper velocity) with $\nabla \cdot \mathbf{v} = 0$
- More spherical and isotropic
- Axial-dispersion dominant over spin-dispersion
- Azimuthal flow u_ϕ strongly dependent on polar angle θ
- Negligible surface energy

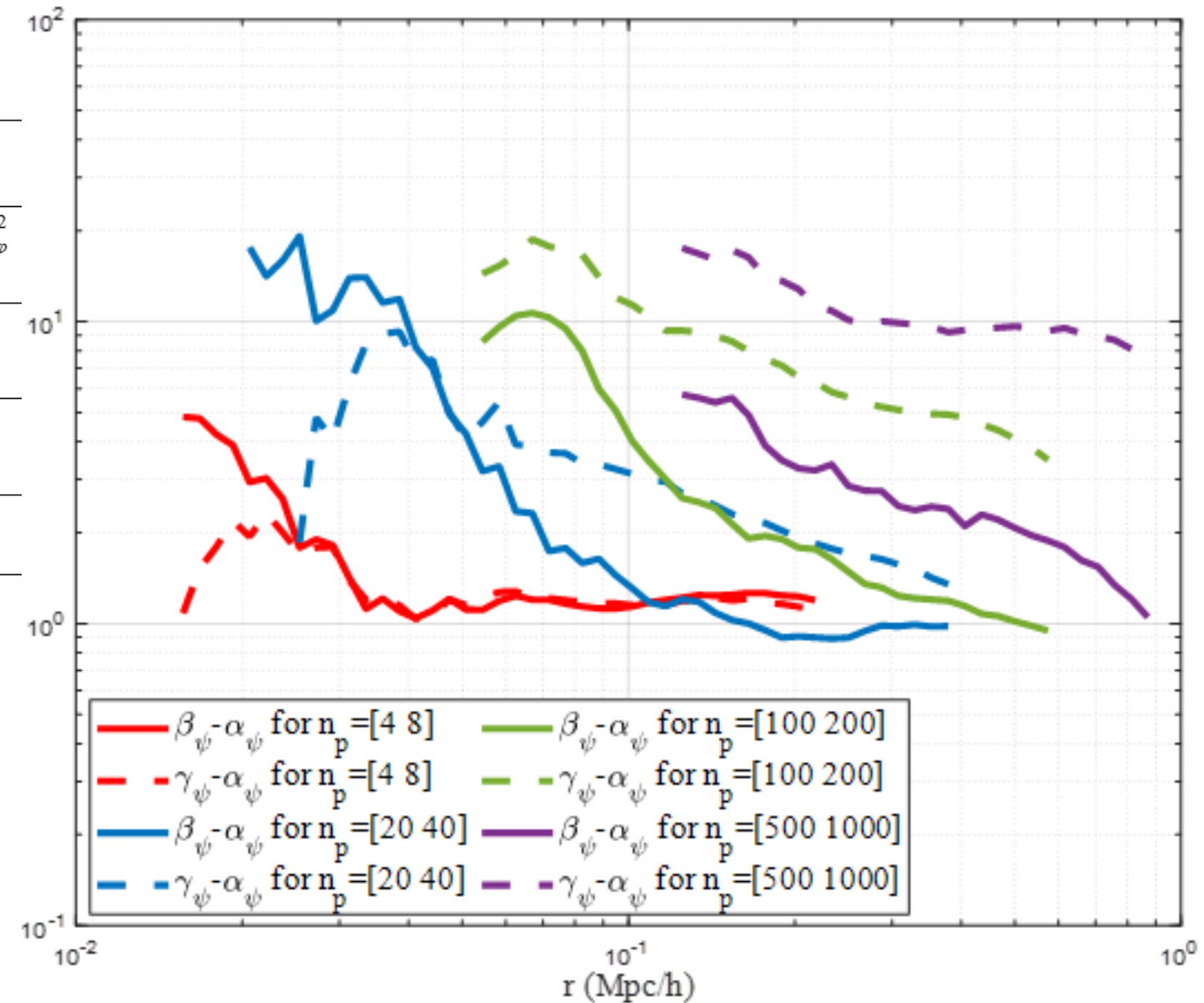


The variation of mean flow and velocity dispersions from N-body simulation

Energy equipartition along three directions

Table 2. Velocity dispersions for rotating and non-rotating halos

		Radial (r)	Azimuthal (φ)	Polar (θ)
Rotating halo (Eq. (9))	Random	$\sigma_{rr}^2 = \sigma_{r0}^2 + 2u_\varphi^2$	$\sigma_{\varphi\varphi}^2 = \sigma_{r0}^2 + 2u_\varphi^2$	$\sigma_{\theta\theta}^2 = \sigma_{r0}^2 + u_\varphi^2$
	Mean flow	0	u_φ^2	0
Non-rotating halo (Eq. (50))	Random	$\sigma_{rr}^2 = \sigma_r^2 = \sigma_{r0}^2$	$\sigma_{\varphi\varphi}^2 = \sigma_{r0}^2$	$\sigma_{\theta\theta}^2 = \sigma_{r0}^2$
	Mean flow	0	0	0



- Due to finite spin, kinetic energy is not equipartitioned along each direction with the greatest energy along the azimuthal direction and the smallest along the polar direction.
- Different from usual objects, halos are hotter with faster spin due to energy transfer between mean flow and random motion.

The variation of dispersion parameters α_φ , β_φ , and γ_φ

Solutions for “large” halos at early stage

Coupling function:

$$F_a(r, t) \approx -\frac{\partial \phi_r}{\partial r}$$

Mean flow:

$$u_\theta = 0$$

Velocity dispersions:

$$\sigma_{rr}^2 = \sigma_{\varphi\varphi}^2 = \sigma_{\theta\theta}^2 + u_\phi^2$$

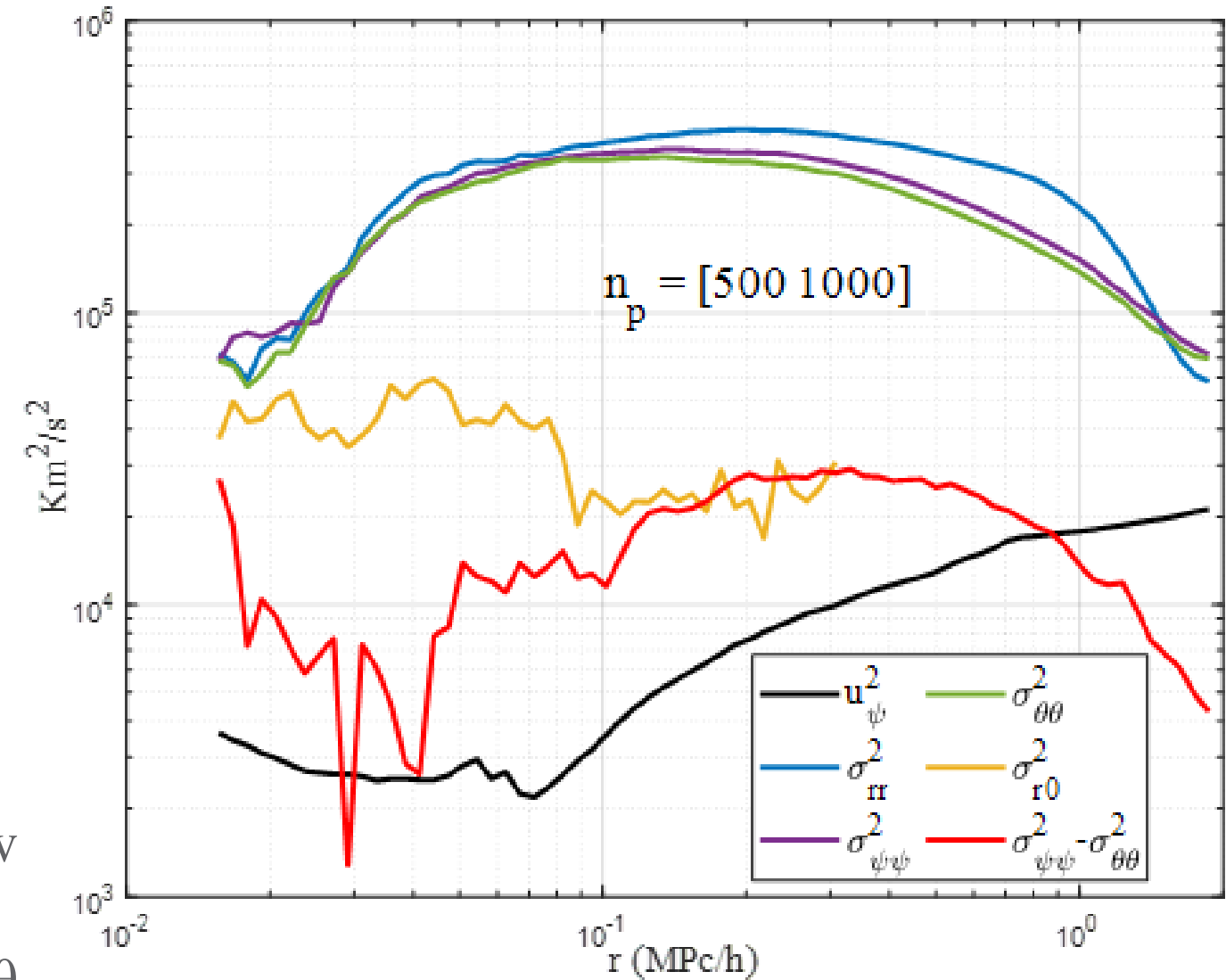
Anisotropy parameters : $\beta_{h1} \approx \beta_h$

Angular exponent : $\alpha_\theta \ll 1$

$$\beta_\varphi = \alpha_\varphi + 1 \quad \alpha_\varphi \gg 1 \quad \gamma_\varphi \approx \alpha_\varphi + 10$$

Properties of “large” halos (continued):

- Non-virialized with non-zero self-similar radial flow
- Spin-dispersion dominant over axial-dispersion
- Azimuthal flow u_φ is less dependent on polar angle θ
- Non-zero surface energy



The variation of mean flow and velocity dispersions from N-body simulation

Solutions for “large” halos at early stage

Radial flow: $u_h(x) = u_r(r) \frac{t}{r_s(t)} = x - \frac{F(x)}{F'(x)}$

Azimuthal flow: $u_\phi(r, \theta, t) = u_\phi(x, \theta) = \alpha_f \omega_h(t) r_s(t) \frac{F(x)}{x}$

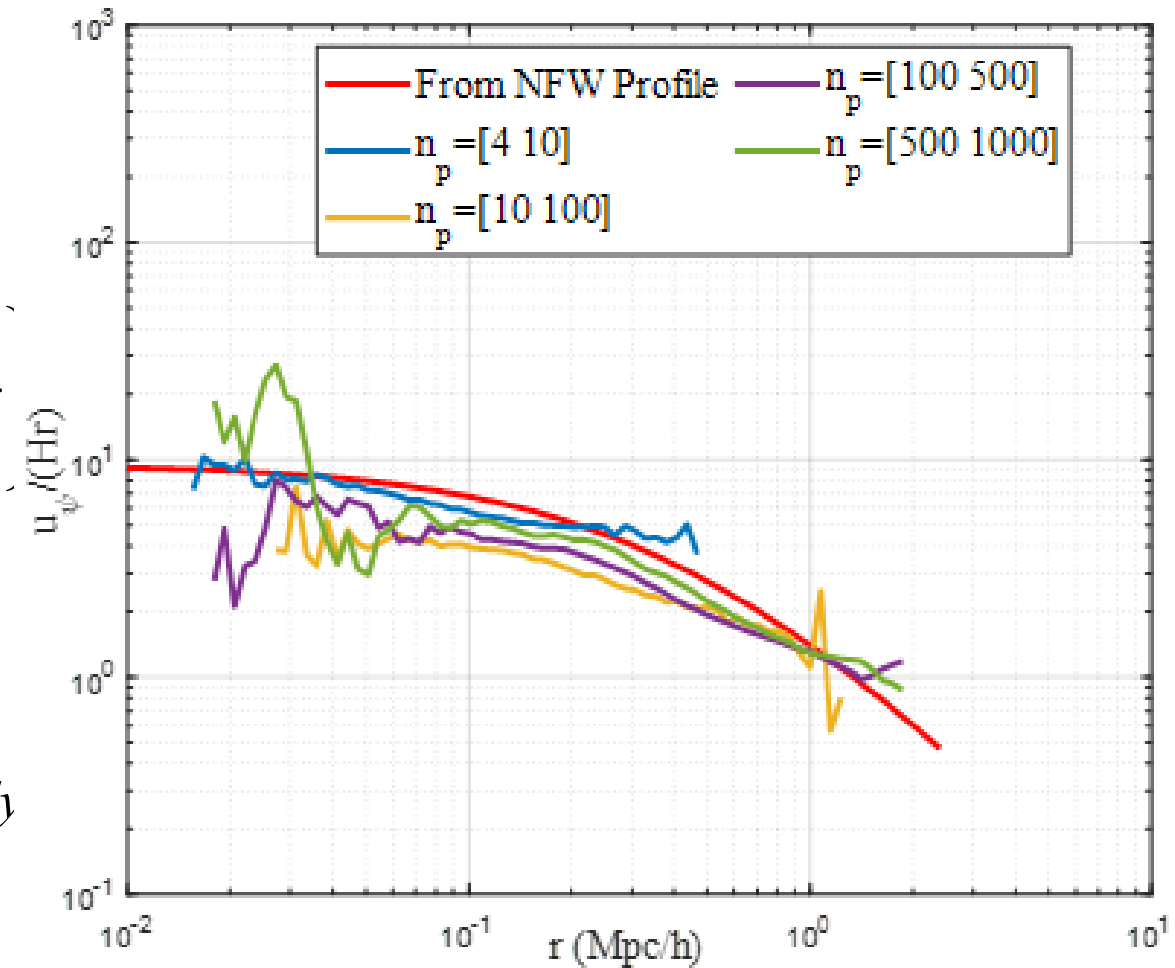
Axial-dispersion: $\sigma_{r0}^2(x) = \frac{v_{cir}^2 x^2}{4\pi^2 c^2 F'(x)} \left\{ \frac{F^2(x)}{x^2 F'(x)} \right\}_x^\infty - \int_x^\infty \left[\frac{2F(x)}{x^2} - \frac{2F^2(x)}{F'(x)x^3} \right] dx$

Angular velocity: $\omega_h = \left(\frac{3}{2\alpha_h} - \frac{1}{2} \right) \frac{c^2}{F(c)\alpha_f} H \propto t^{-1}$ and $\alpha_f = \frac{16c^2}{3\pi F(c)} \gamma_g^2$

Dispersion parameter: $\gamma_\phi(x) = \frac{x^4}{F^2(x)F'(x)} \left[18 \int_x^\infty \frac{F^2(y)F'(y)}{y^5} dy + \lambda_f \int_x^\infty \frac{F(y)F'(y)}{y^4} dy \right]$

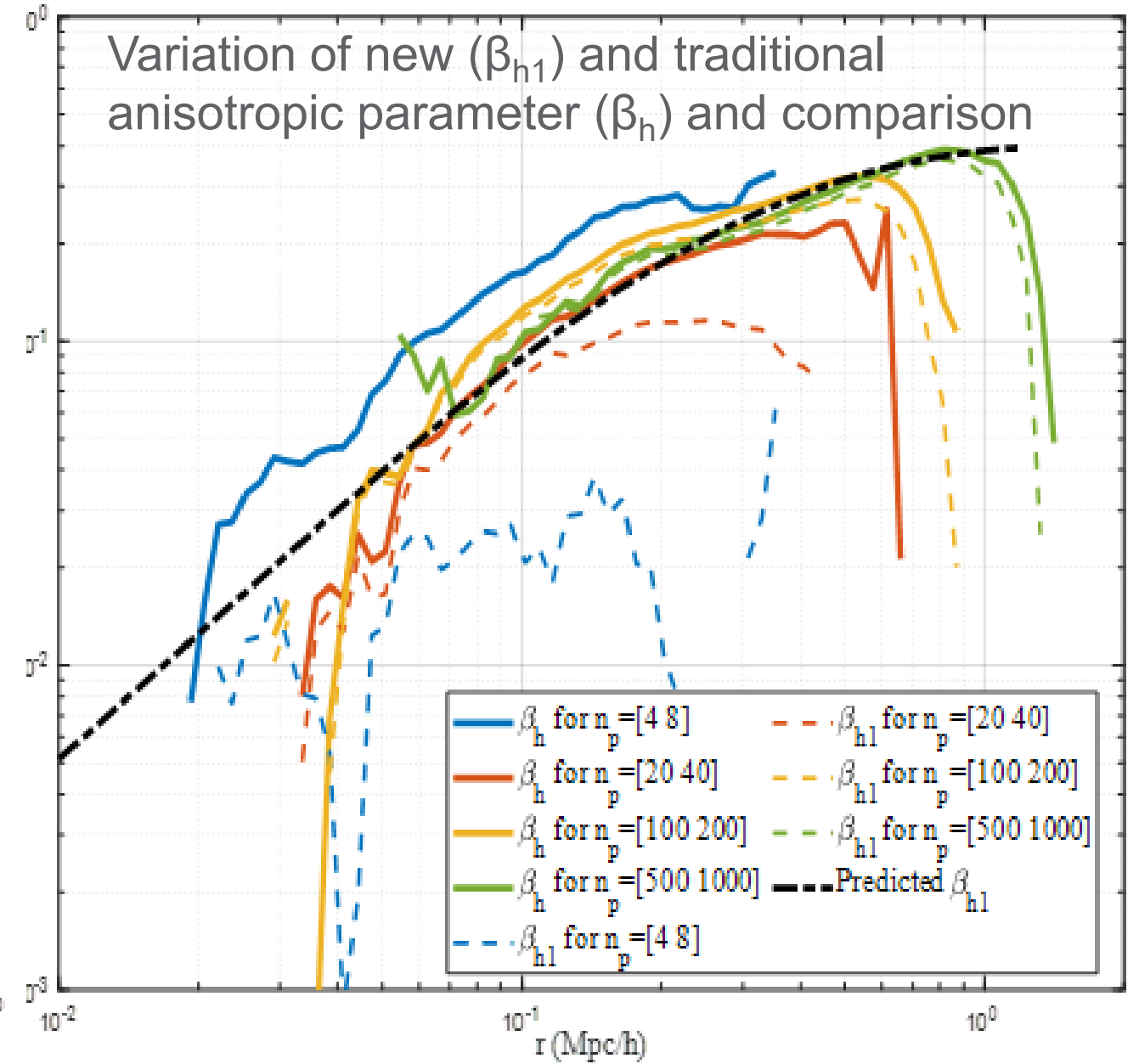
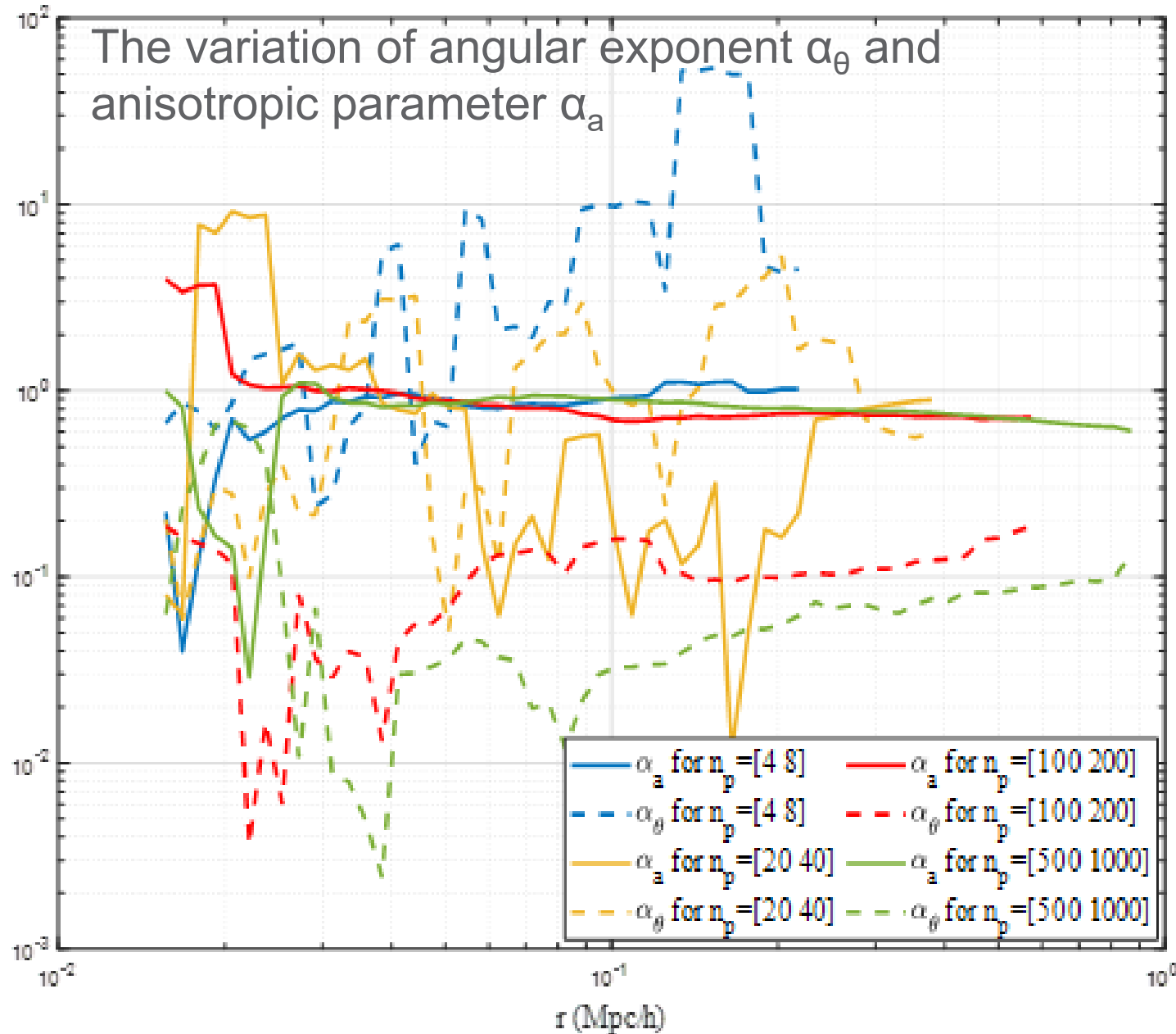
$$\lambda_f = \frac{9\pi^2 F(c)}{(3/(2\alpha_h) - 1/2)^2 c} \quad \beta_\phi = \alpha_\phi + 1 \quad \text{and} \quad \gamma_\phi \approx \alpha_\phi + 10$$

Deformation parameter: α_h Anisotropic parameters: $\alpha_a = \frac{(\alpha_\phi + \beta_\phi + 1)}{2\gamma_\phi}$ $\beta_{h1} = \frac{1 - \alpha_a}{1 + \sigma_{r0}^2 / (\gamma_\phi u_\phi^2)}$



The variation of azimuthal flow from N-body simulation and comparison

Angular exponent and anisotropic parameters



Halo momentum and energy in terms of $F(x)$

Mean square radius:

$$r_g^2 = \frac{1}{m_h} \int_0^{r_h} 4\pi r^2 \rho_h(r) r^2 dr = r_h^2 \left[1 - \frac{2}{c^2 F(c)} \int_0^c x F(x) dx \right] = \gamma_g^2 r_h^2$$

(physical)

radial linear momentum:
$$L_h = \frac{1}{m_h} \int_0^{r_h} 4\pi r^2 \rho_h u_r dr = \frac{3}{2} \left(1 - \frac{2}{c F(c)} \int_0^c F(x) dx \right) H r_h$$

(peculiar)

radial linear momentum:
$$L_{hp} = \frac{1}{m_h} \int_0^{r_h} 4\pi r^2 \rho_h u_{rp} dr = \frac{1}{2} \left(1 - \frac{4}{c F(c)} \int_0^c F(x) dx \right) H r_h$$

(physical)
virial quantity:

$$G_h = \frac{1}{m_h} \int_0^{r_h} 4\pi r^3 \rho_h u_r dr = \frac{3}{2} \left[1 - \frac{3}{c^2 F(c)} \int_0^c x F(x) dx \right] H r_h^2$$

(peculiar)
virial quantity:

$$G_{hp} = \frac{1}{m_h} \int_0^{r_h} 4\pi r^3 \rho_h u_{rp} dr = \frac{1}{2} \left[1 - \frac{5}{c^2 F(c)} \int_0^c x F(x) dx \right] H r_h^2$$

Angular momentum:

$$H_h = \left(\frac{1}{\alpha_h} - \frac{1}{3} \right) \frac{c^2}{F(c) \alpha_f} (G_h - G_{hp}) = \left(\frac{1}{\alpha_h} - \frac{1}{3} \right) \frac{c^2}{F(c) \alpha_f} H r_g^2$$

Moment of inertia:

$$I_\omega = \frac{2}{3} m_h r_g^2$$

Angular momentum:

$$H_h = \frac{2}{3} \omega_h r_g^2$$

Specific momentum tensor:

$$\frac{1}{m_h} \int_V \mathbf{x} \otimes \mathbf{u}_p \rho_h dV = \begin{bmatrix} G_{hp}/3 & -H_h/2 & 0 \\ H_h/2 & G_{hp}/3 & 0 \\ 0 & 0 & G_{hp}/3 \end{bmatrix}$$

(physical)

radial kinetic energy:
$$K_r = \frac{1}{2m_h} \int_0^{r_h} u_r^2(r, a) 4\pi r^2 \rho_h(r, a) dr$$

(peculiar)

radial kinetic energy:
$$K_{rp} = \frac{1}{2m_h} \int_0^{r_h} u_{rp}^2 4\pi r^2 \rho_h(r, a) dr$$

Rotational kinetic energy:

$$K_a = \frac{1}{m_h} \int_0^{r_h} 2\pi r^3 \rho_h(r) \left(\int_0^\pi \frac{1}{2} u_\phi^2 \sin \theta d\theta \right) dr$$

Halo spin parameters in terms of F(x)

Two definitions of spin parameters:

$$\lambda_p = \frac{H_h |E_h|^{1/2}}{Gm_h} \quad \text{and} \quad \lambda'_p = \frac{H_h}{\sqrt{2}v_{cir}r_h}$$

Mean square
radius:

$$r_g = \gamma_g r_h = \gamma_g a \left(\frac{2Gm_h}{\Delta_c H_0^2} \right)^{1/3}$$

Halo (specific) energy and angular momentum:

$$E_h = \Phi_h + K_h \quad \text{and} \quad H_h = \gamma_H H r_h^2$$

Virial
dispersion:

$$\sigma_v^2 = -\Phi_h \frac{\gamma_v}{3} = \frac{1}{3} \gamma_\Phi \gamma_v \left(\frac{\Delta_c}{2} \right)^{1/3} (Gm_h H_0)^{2/3} a^{-1}$$

Halo (specific) potential energy:

$$\Phi_h = -\gamma_\Phi \frac{Gm_h}{r_h} = -\frac{1}{m_h} \int_0^{r_h} 4\pi r^2 \rho_h(r, a) \frac{Gm_r}{r} dr = -\frac{1}{2} \gamma_\Phi \Delta_c H^2 r_h^2 \quad \text{and} \quad \gamma_\Phi = \left(\frac{c}{F^2(c)} \int_0^c \frac{F(x)F'(x)}{x} dx \right) \approx 1$$

Halo (specific) kinetic energy and rotational kinetic energy:

$$K_h = 3/2 \sigma_v^2 = (n_e/2) \Phi_h \quad \text{and} \quad K_a \approx \frac{1}{2} |\mathbf{H}_h| \omega_h = \frac{3}{4} (|\mathbf{H}_h|/r_g)^2$$

Circular
velocity: $v_{cir} = \sqrt{\Delta_c/2} H r_h = 3\pi H r_h$

$$\lambda_p = \gamma_\Phi \gamma_g \sqrt{\frac{4}{3} \left(1 + \frac{n_e}{2}\right) \frac{K_a}{|\Phi_h|}} = \frac{2}{3} \gamma_\Phi \gamma_g \sqrt{\gamma_v \left(1 - \frac{\gamma_v}{2}\right) \frac{K_a}{\sigma_v^2}} \rightarrow \lambda_p = \frac{\gamma_H}{3\pi} \sqrt{\gamma_\Phi \left(1 + \frac{n_e}{2}\right)} \approx 0.031$$

$$\lambda'_p = \gamma_g \sqrt{\frac{2\gamma_\Phi K_a}{3|\Phi_h|}} = \frac{1}{3} \gamma_g \sqrt{2\gamma_\Phi \gamma_v \frac{K_a}{\sigma_v^2}} \rightarrow \lambda'_p = \frac{\gamma_H}{3\pi\sqrt{2}} \approx 0.038$$

Spin parameters
reflects the ratio
between rotational and
virial kinetic energy

Energy, momentum and spin parameter for NFW and isothermal halos

Table 3. Relevant parameters for two different density profiles

Symbol	Physical meaning	Equation	Isothermal profile with $\alpha_\theta = 1$	NFW profile with $\alpha_\theta = 0$ and $c = 3.5$
$F(x)$	Function for density ρ_h	Eq. (33)	x/c	$\ln(1+x) - x/(1+x)$
α_h	Deformation parameter	Eq. (66)	1.0	0.833
γ_h	Deformation rate parameter	Eq. (69)	0	1/2
α_f	Constant for function $F_\phi(x)$	Eq. (77)	$2c^2/3$	9.20
λ_f	Constant for equation for γ_ϕ	Eq. (92)	$9\pi^2/c$	10.895
γ_H	Coefficient for H_h	Eq. (106)	1/3	0.511
γ_Φ	Coefficient for potential Φ_h	Eq. (113)	1	0.936
γ_v	Virial ratio	Eq. (115)	1.5	1.3
$\gamma_g^2 = r_g^2/r_h^2$	Ratio of two halo sizes	Eq. (73)	1/3	0.3214
L_h	Specific radial momentum	Eq. (100)	0	0
L_{hp}	Peculiar radial momentum	Eq. (101)	$-Hr_h/2$	$-0.501Hr_h$

Table 3. Relevant parameters for two different density profiles

Symbol	Physical meaning	Equation	Isothermal profile with $\alpha_\theta = 1$	NFW profile with $\alpha_\theta = 0$ and $c = 3.5$
G_h	Specific virial quantity	Eq. (102)	0	$-0.027Hr_h^2$
G_{hp}	Peculiar virial quantity	Eq. (103)	$-Hr_h^2/3$	$-0.348Hr_h^2$
H_h	Specific angular momentum	Eq. (105)	$Hr_h^2/3$	$0.511Hr_h^2$
ω_h	Angular velocity	Eq. (81)	$1.5H$	$2.38H$
K_r	Radial kinetic energy	Eq. (108)	0	$0.0062H^2r_h^2$
K_{rp}	Peculiar radial kinetic energy	Eq. (109)	$H^2r_h^2/6$	$0.1937H^2r_h^2$
K_a	Rotational kinetic energy	Eq. (110)	$H^2r_h^2/3$	$0.7658H^2r_h^2$
Φ_h	Halo potential energy	Eq. (112)	$-9\pi^2H^2r_h^2$	$-8.424\pi^2H^2r_h^2$
λ_p	First halo spin parameter	Eq. (119)	0.018	0.031
λ'_p	Second halo spin parameter	Eq. (119)	0.025	0.038

The energy transfer between mean flow and random flow in “large” high v halos

Two contributions for change of halo momentum /energy:

S1: Bulk contribution from internal exchange between mean flow and random flow

S2: Surface contribution from mass cascade

Example:

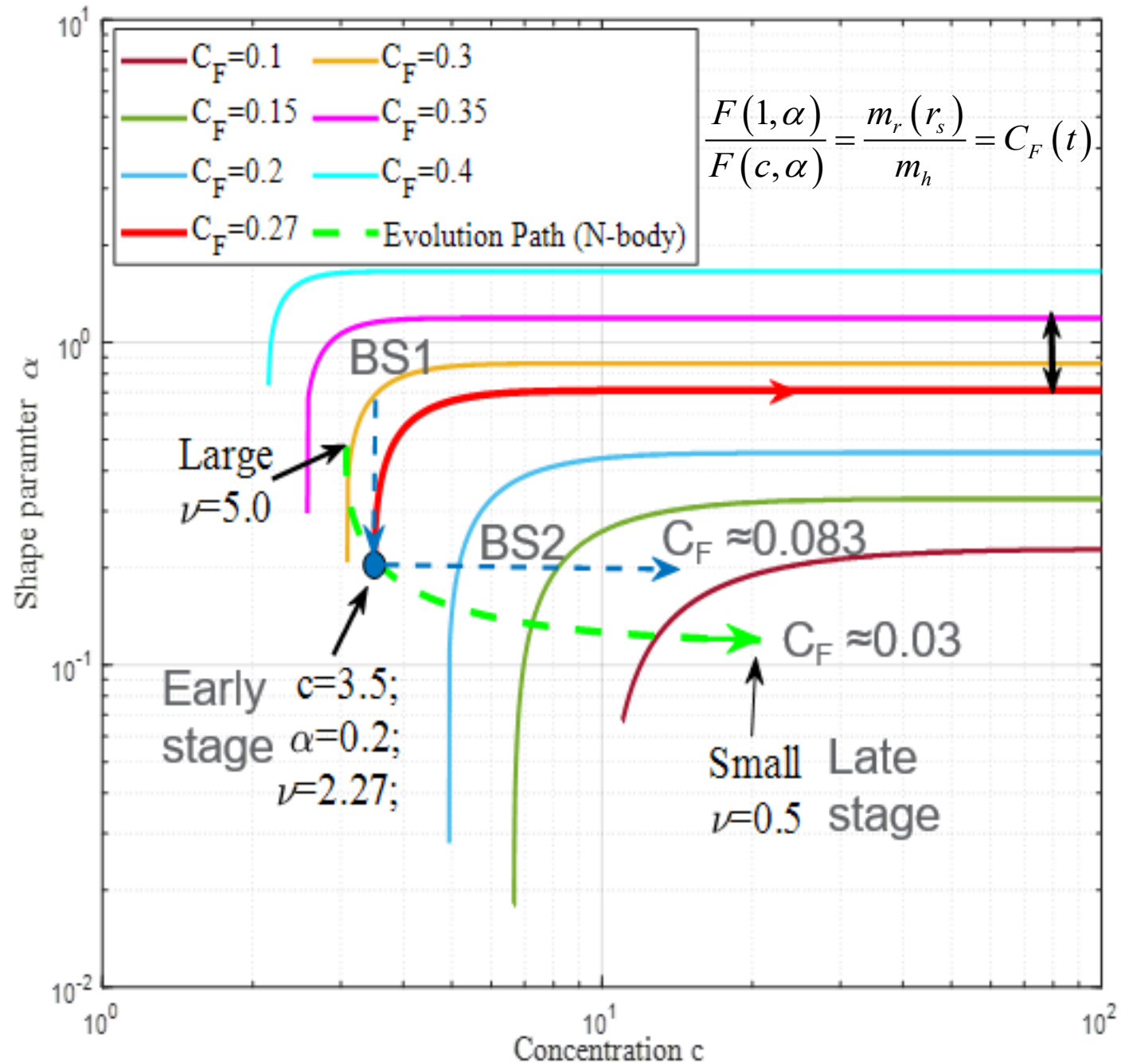
$$\frac{\partial \bar{L}_h}{\partial t} = \frac{m_h r_h}{t^2} \left[\underbrace{\left(1 - \frac{1}{\alpha_h}\right)}_{S_2} + \underbrace{\left(\frac{1}{\alpha_h} - \frac{2}{cF(c)} \int_0^c F(x) dx\right)}_{S_1} \right]$$

- For angular momentum, all contributions from S2, i.e. mass cascade.
- For radial kinetic energy, two contributions are comparable.
- For rotational kinetic energy, contribution from S2 is dominant, i.e. mass cascade.
- In addition, local energy transfer can be **two-way**. S1 < 0 for entire halo, **one-way** net kinetic energy is transferred from mean flow to random motion to enhance halo entropy.

Table 4. The rate of change of halo momentum and energy for two different density profiles

Symbol	Physical meaning	Isothermal with $\alpha_\theta = 0$	NFW profile $\alpha_\theta = 0; c = 3.5$
$\partial \bar{L}_h / \partial t$	radial momentum	0	0
S_1	Bulk contribution	0	$0.2 m_h r_h / t^2$
S_2	Surface contribution	0	$-0.2 m_h r_h / t^2$
$\partial \bar{H}_h / \partial t$	angular momentum	$\frac{\pi m_h H r_h^2}{4 t}$	$\frac{\pi m_h H r_h^2}{4 t} \left(\frac{3}{2\alpha_h} - \frac{1}{2} \right)$
S_1	Bulk contribution	0	0
S_2	Surface contribution	$\frac{\pi m_h H r_h^2}{4 t}$	$\frac{\pi m_h H r_h^2}{4 t} \left(\frac{3}{2\alpha_h} - \frac{1}{2} \right)$
$\partial \bar{K}_r / \partial t$	radial kinetic energy	0	$0.0062 H^2 r_h^2 m_h / t$
S_1	Bulk contribution	0	$-0.0391 H^2 r_h^2 m_h / t$
S_2	Surface contribution	0	$0.0453 H^2 r_h^2 m_h / t$
$\partial \bar{K}_{rp} / \partial t$	peculiar radial kinetic energy	$H^2 r_h^2 m_h / (6t)$	$0.1937 H^2 r_h^2 m_h / t$
S_1	Bulk contribution	$-H^2 r_h^2 m_h / (3t)$	$-0.6525 H^2 r_h^2 m_h / t$
S_2	Surface contribution	$H^2 r_h^2 m_h / (2t)$	$0.8462 H^2 r_h^2 m_h / t$
$\partial \bar{K}_a / \partial t$	rotational kinetic energy	$H^2 r_h^2 m_h / (2t)$	$0.7661 H^2 r_h^2 m_h / t$
S_1	Bulk contribution	0	$-0.0801 H^2 r_h^2 m_h / t$
S_2	Surface contribution	$H^2 r_h^2 / 2$	$0.8462 H^2 r_h^2 m_h / t$

Halo relaxation (stretching) from early to late stages



- Two-parameter Einasto profile for relaxation
- The path of evolution in c - α space (shape parameter vs. concentration)
- Contour for constant core/halo mass ratio C_F
- Evolution path from N-body simulation (green)
- Simplified path for analytical calculation (blue)
 - Blue segment 1 (BS1): constant $c \approx 3.5$
 - Blue segment 2 (BS2): constant $\alpha \approx 0.2$
- Path to composite halos with $\alpha \approx 0.7$ (red) follows a constant $C_F = 0.27$; Adiabatic process
- Goal: explore the continuous variation of halo shape, density profile, mean flow, momentum, and energies during halo relaxation.

Decomposition of radial flow

Extend key function $F(x)$ to two-parameter function $F(x, \alpha)$, where α is a shape parameter:

$$\rho_h(r, t) = \frac{1}{4\pi r^2} \frac{\partial m_r(r, a)}{\partial r} = \frac{m_h(t)}{4\pi r_s^3} \frac{F'(x, \alpha)}{x^2 F(c, \alpha)} \quad \text{Enclosed mass: } m_r(r, t) = m_h(t) \frac{F(x, \alpha)}{F(c, \alpha)}$$

$$\frac{\partial \rho_h(r, a)}{\partial t} = \frac{1}{4\pi r^2} \frac{\partial^2 m_r(r, a)}{\partial r \partial t} \quad \frac{\partial m_r(r, a)}{\partial t} = -4\pi r^2 u_r(r, a) \rho_h(r, a) \quad (\text{From continuity equation})$$

$$u_h = u_{hm} + u_{hc} + u_{h\alpha}$$

From mass cascade:

$$u_{hm} = x \frac{\partial \ln r_s}{\partial \ln t} - \frac{F(x, \alpha)}{F'(x, \alpha)} \frac{\partial \ln m_h}{\partial \ln t}$$

From conc. change:

$$u_{hc} = \frac{\partial \ln c}{\partial \ln t} \frac{F(x, \alpha)}{F'(x, \alpha)} \frac{\partial \ln F(c, \alpha)}{\partial \ln c}$$

From shape change:

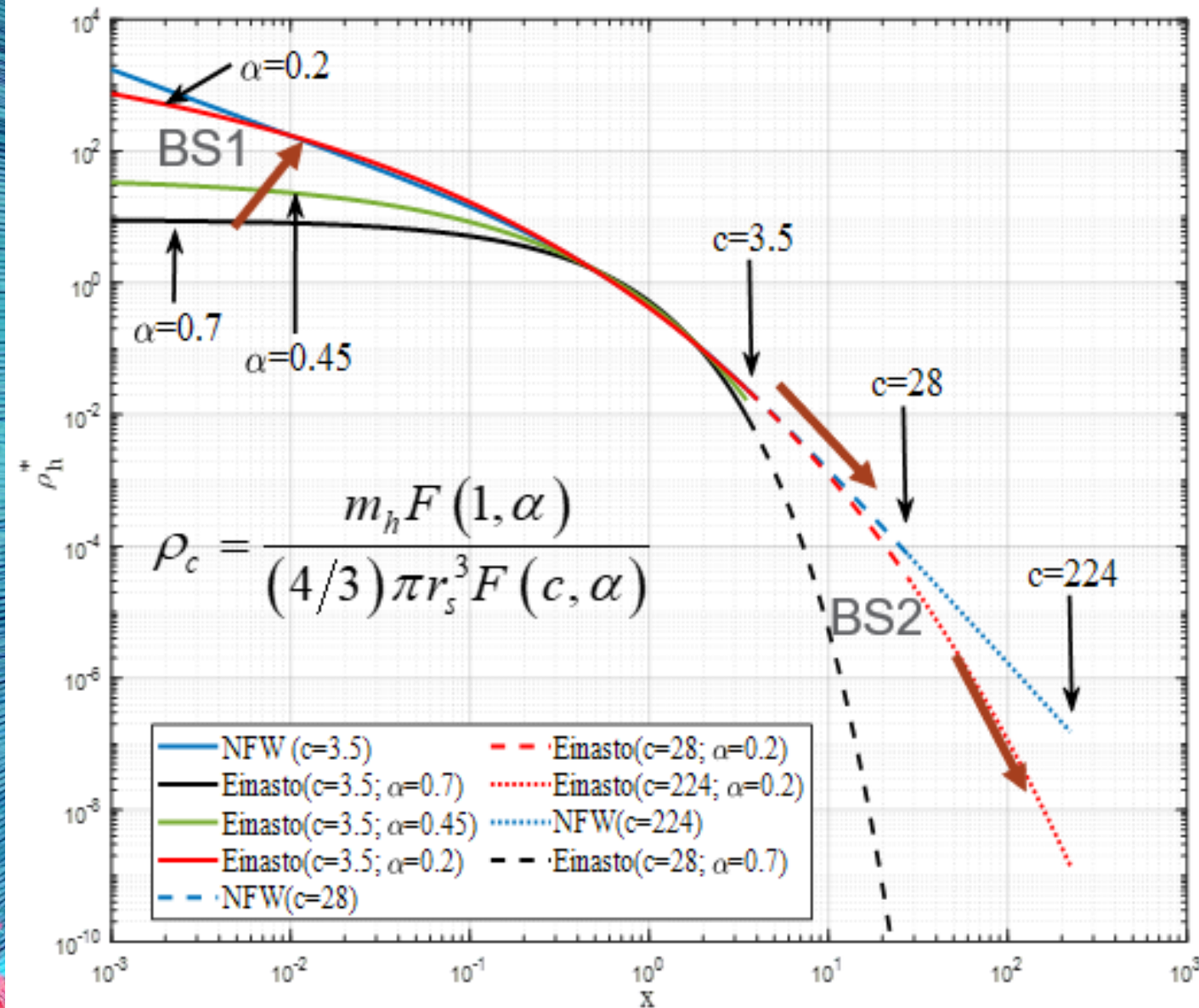
$$u_{h\alpha} = \frac{\partial \ln \alpha}{\partial \ln t} \frac{F(x, \alpha)}{F'(x, \alpha)} \left[\frac{\partial \ln F(c, \alpha)}{\partial \ln \alpha} - \frac{\partial \ln F(x, \alpha)}{\partial \ln \alpha} \right]$$

- Early stage “large” halos: $u_{hc}=0$ and $u_{h\alpha}=0$ radial flow from cascade u_{hm} is dominant;

- Late stage “small” halos: all three radial flows vanishes and $u_h=0$;

- For halo “relaxation” from early to late stage (BS2), we expect a constant r_s , constant α , $m_h \sim F(c, \alpha)$, $u_{h\alpha}=0$, and $u_{hm} + u_{hc} = 0$

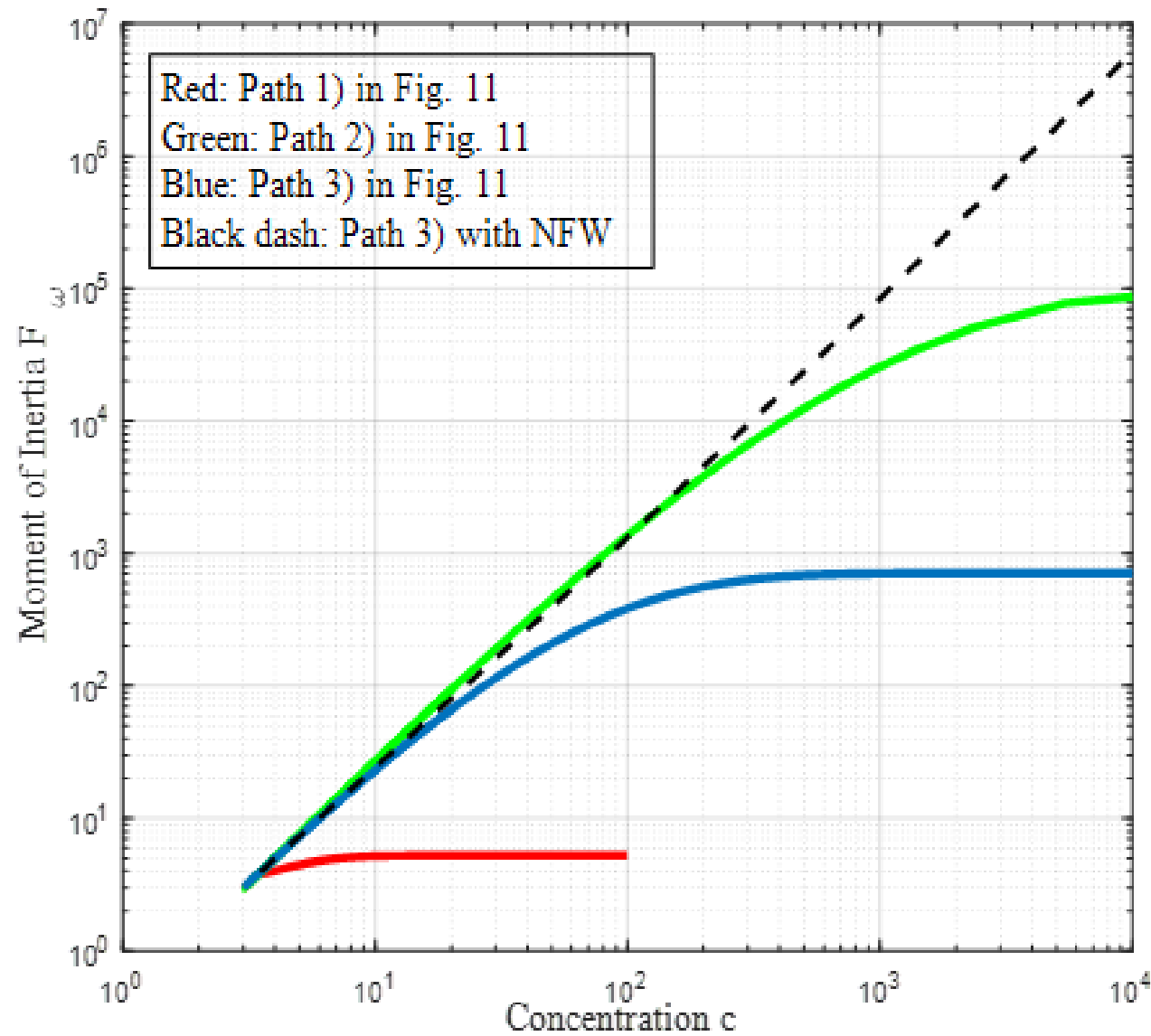
Density profile from early to late stages



Variation of halo density normalized by the average core density ρ_c (with $r < r_s$)

- During BS1 with constant $c \approx 3.5$ and constant C_F , decreasing α involves significant change of density in halo core, i.e. steeper density slope and increasing core mass.
- During BS2 with constant $\alpha \approx 0.2$, increasing c involves a stable core (constant scale radius r_s , constant core mass, and core density ρ_c) and extending halo skirt (“halo stretching” vs. “vortex stretching” in turbulence).
- **Vortex stretching: anisotropic, volume conserving, constant density, and decreasing momentum of inertia.**
- **Halo stretching: isotropic, increasing volume, varying density, and increasing momentum of inertia.**

Moment of inertia from early to late stage



Variation of moment of inertia with concentration c

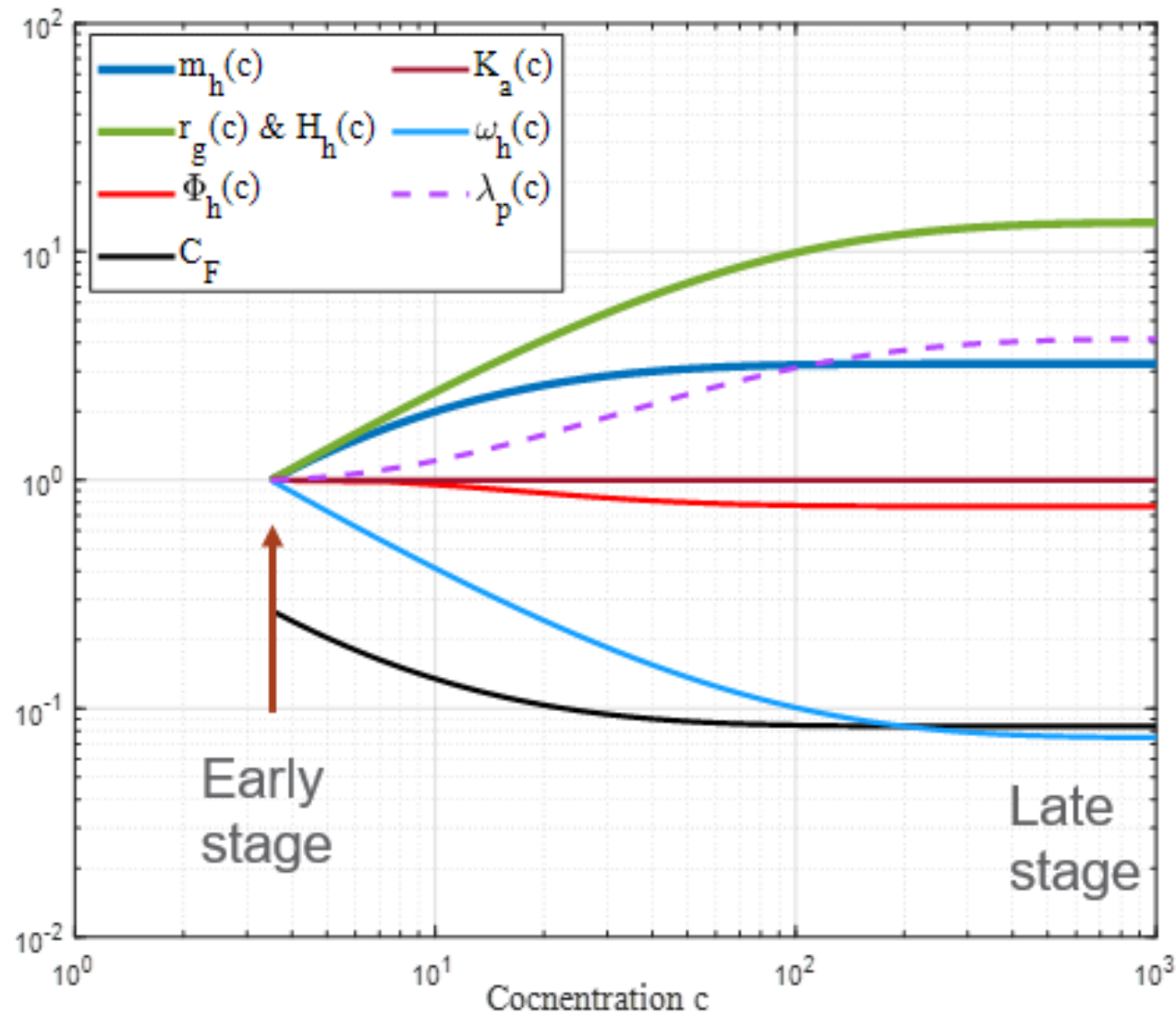
Moment of inertia:
$$I_{\omega} = \frac{2}{3} m_h r_g^2 = \frac{2}{3} m_h r_s^2 F_{\omega}(\alpha, c)$$

Mean square radius:
$$r_g(c) = r_s \sqrt{F_{\omega}(c)}$$

$$F_{\omega}(\alpha, c) = \left(\frac{\alpha}{2}\right)^{\frac{2}{\alpha}} \frac{\Gamma(5/\alpha) - \Gamma(5/\alpha, 2c^{\alpha}/\alpha)}{\Gamma(3/\alpha) - \Gamma(3/\alpha, 2c^{\alpha}/\alpha)}$$

- Red path is adiabatic with constant halo mass, with both angular momentum and rotational energy conserved.
- Green path from simulation shows significant increase in moment of inertia from halo “stretching”.
- Simplified blue path with constant r_s and core mass shows the increase in moment of inertia that plateaus at large c .

Variation of mass, moment, energy during relaxation



Variation of halo momentum and energies during halo relaxation

Specific rotational kinetic energy: $K_a = \frac{1}{2} |\mathbf{H}_h| \omega_h = \frac{3}{4} (|\mathbf{H}_h| / r_g)^2$

Specific angular momentum: $|\mathbf{H}_h| = \frac{2}{3} \omega_h r_g^2$ λ_p : spin parameter

For early stage “large” halos:

$\lambda_p \approx 0.031$ $m_h \propto t$ $|\mathbf{H}_h| \propto t$ $K_a \propto t^0$ Spin-dispersion dominant
 $C_F = 0.27$ $r_g \propto t$ $\omega_h \propto t^{-1}$ $\Phi_h \propto t^0$ dominant

For late stage “small” halos:

$\lambda_p \approx 0.124$ $m_h \propto t^0$ $|\mathbf{H}_h| \propto t^0$ $K_a \propto t^0$ Axial-dispersion dominant
 $C_F = 0.083$ $r_g \propto t^0$ $\omega_h \propto t^0$ $\Phi_h \propto t^0$ dominant

- Halo “relaxation” (via BS2): with constant $\alpha \approx 0.2$, increasing c , constant r_s , core mass, and core density
- Specific rotational kinetic energy is relatively conserved
- $|\mathbf{H}_h| \propto r_g$ $\omega_h \propto r_g^{-1}$
- Spin-dispersion dominant to axial-dispersion dominant

Summary and keywords

Early stage “large” halos	Late stage “small” halos	Core mass ratio	Axial dispersion
Vortex stretching	Halo stretching	Fictitious stress	Spin dispersion
Path of halo evolution “relaxation”	<u>Radial flow decomposition</u>	Energy transfer	

- Review one-way energy transfer via vortex stretching in turbulence;
- Halos enable a two-way energy transfer between mean flow and random motion;
- Analytical solutions of mean flow, velocity dispersion, and anisotropy parameters for halos at their early stage and late stage using decomposition of velocity dispersion.
- “Early-stage” halos have their mass, size, kinetic/potential/rotational energy, and the specific angular momentum all increase linearly with time via continuous mass acquisition. Halo core spins faster than the outer region.
- “Late-stage” halos are more spherical in shape, incompressible, and isotropic. Due to finite halo spin, kinetic energy is not equipartitioned along each direction with the greatest energy along the azimuthal direction. Halos are hotter with faster spin.
- Identify the path of relaxation via halo stretching for halos relaxing from early to late stage involving continuous variation of shape, density profile, mean flow, momentum, and energy.
- Might extend to consider effect of black hole at halo center on radial flow